

## On the Decelerating Shock Instability of Plane-Parallel Slab with Finite Thickness

RYOICHI NISHI<sup>1</sup> and HIDEYUKI KAMAYA<sup>1,2</sup>

1 : Department of Physics, Kyoto University, Sakyo-ku, Kyoto 606-8502, JAPAN

2 : Department of Astronomy, Kyoto University, Sakyo-ku, Kyoto 606-8502, JAPAN

email(RN):nishi@tap.scphys.kyoto-u.ac.jp

email(HK):kamaya@kusastro.kyoto-u.ac.jp

Apr. 16th, 1999

### ABSTRACT

Dynamical stability of the shock compressed layer with finite thickness is investigated. It is characterized by self-gravity, structure, and shock condition at the surfaces of the compressed layer. At one side of the shocked layer, its surface condition is determined via the ram pressure, while at the other side the thermal pressure supports its structure. When the ram pressure dominates the thermal pressure, we expect deceleration of the shocked layer. Especially, in this paper, we examine how the stratification of the decelerating layer has an effect on its dynamical stability. Performing the linear perturbation analysis, a *more general* dispersion relation than the previous one obtained by one of the authors is derived. It gives us an interesting information about the stability of the decelerating layer; When the deceleration of the layer dominates the self-gravity, the so-called DSI (Decelerating Shock Instability) is efficient, while the gravitational instability occurs when the self-gravity works better than the deceleration. The length-scales of the two instabilities are the order of the width of the decelerating layer. Their growth time-scales are the order of the free-fall time in the density of the shocked slab. Importantly, they are always incompatible. We also consider the evolution effect of the shocked layer. In the early stages of its evolution, only DSI occurs. On the contrary, in the late stages, it is possible for the shocked layer to be unstable for the DSI (in smaller scale) and the gravitational instability (in larger scale), ordinary. The onset-time of the gravitational instability is the order of the free-fall time of the external medium. After onset, as shown above, growth time-scale becomes the free-fall time of the dense slab, which is much shorter than the free-fall time of the external

medium. Furthermore, we find there is a stable range of wavenumbers against both the DSI and the gravitational instability between respective unstable wavenumber ranges. These stable modes suggest the ineffectiveness of DSI for the fragmentation of the decelerating slab. Thus, in various cases, the structure of the shocked layer should be determined when its stability is discussed.

*Subject headings:* hydrodynamics — instabilities — shock waves — stars:formation

## 1. INTRODUCTION

The hydrodynamic shock waves are expected to play important roles in many astrophysical phenomena, especially in the formation of the structure. The shock waves are induced by supernovae (e.g. Tomisaka 1990), expanding H<sub>II</sub> regions (e.g. Elmegreen 1989), molecular outflows around protostars (e.g. Nakano, Hasegawa, & Norman 1995), stellar winds from early type stars (e.g. Stevens, Blondin, & Pollock 1992), and so on. These expanding shock waves sweep up the external matter and the swept matter will become the materials of the structure at the next stage (e.g. Kimura & Tosa 1988). Previously, it was postulated that such mechanism performs in the galaxy formation era (e.g. Ikeuchi 1981). In this paper, paying attention to the finite thickness of the shocked layer (cf. Vishniac & Ryu 1989), we reexamine its stability by linear perturbation analysis. Especially, we present a general dispersion relation including the effect of the self-gravity of a shocked slab with finite thickness.

The stability of decelerating shock waves have been investigated, especially in the last two decades. Vishniac (1983) firstly studies the isothermal shock waves expanding spherically in a uniform medium with a thin shell picture. Then, he has found that it is overstable against linear perturbations and the smaller wavelength perturbation is more unstable, although plane shock waves in a steady state were believed to be stable for rippling perturbation (Erpenbeck 1962). His instability is attendant on the decelerating shock waves (e.g. Nishi 1992). Then, we shall call it DSI (Decelerating Shock Instability). Importantly, after his series of papers (Ryu & Vishniac 1987, 1988, 1991 Vishniac & Ryu 1989) is published, Grun et al. (1991) has reported the existence of instability of shock wave in laboratory. After that, Mac Low & Norman (1993) study the nonlinear evolution of the blast waves, and confirm Grun et al.. The self-gravity effect on non-linear stage is examined numerically by Yoshida & Habe (1992). Dgani, van Buren & Noriega-Crespo (1996) also discuss the stability of bow-shocks by means of the numerical simulations, and

the transverse acceleration instability semi-analytically. The evolution of the supernova remnant is discussed in Chevalier & Blondin (1995). Vishniac (1994) examines the stability of a slab bounded on both sides by shocks, which is linearly stable but nonlinearly unstable. His analysis is confirmed by numerical simulations (Blondin & Marks 1996). For the extended review, see Vishniac (1995).

There is an important astrophysical phenomenon related to the decelerating shock waves. Elmegreen and Lada (1977) propose a scenario on sequential formation of OB star subgroups. According to their scenario, an H<sub>II</sub> region formed by a group of OB stars expands in a molecular cloud and a shock wave sweeps up the gas. Afterwards, the matter swept up by the shock becomes gravitationally unstable and fragmentation occurs. Elmegreen and Elmegreen (1978) studies the stability of the isothermal layer supported by the thermal pressure on both sides and showed that the layer is gravitationally unstable and the growth rate has the maximum for the perturbation wavelength several times the thickness of the layer. The case of the high external pressure to the self-gravity is examined by Lubow & Pringle (1993). Welter (1982) calculates the growth rate of the perturbation in the layer which is supported by thermal pressure on one side and by balancing ram pressure of the shock on the other side. Voit (1988) investigates the incompressible sheet supported by unbalanced two thermal pressures and shows the coupling of the gravitational instability and the Rayleigh-Taylor instability. The effect of the magnetic field to the stability of the self-gravitating slab is precisely examined by Nagai, Inutsuka, & Miyama (1998).

However, importantly, the shock-compressed layers around H<sub>II</sub> regions are supported by the thermal pressure on one side and the ram pressure on the other side, and the two pressures are not always balanced. In this work, we expect that the instability related to a decelerating shock wave plays an important role. Moreover, we must study the instability of the shocked self-gravitating layers, since in the scenario of sequential star formation the next generation of OB stars is finally formed by self-gravity. Elmegreen (1989) calculates the evolution of an isothermal shocked layer and the growth of the perturbations in the evolving dense layer with self-gravity. The estimated growth time-scale is  $\sim 0.25(G\rho_e)^{-1/2}$ , and is insensitive to the Mach number. Here  $\rho_e$  is the density of the external (preshock) medium. On the contrary, Vishniac (1983) estimates a relatively short scale and small mass scale for gravitational collapse, which are essentially determined by postshock density. Nishi (1992)'s estimate is resemble to Vishniac (1983). The discrepancy originates from the fact that they adopt different approximation in their analyses each other. As pointed out by Mac Low & Norman (1993), one of the differences is that Vishniac (1983) assumes trans-sonic turbulence in the shell, while Elmegreen (1989) assumes supersonic turbulence with Mach number close to the shock velocity, and Mac Low & Norman's numerical work, in which gravity is neglected, may support Vishniac's assumption. Moreover, very importantly, the

structure of the shocked slab are not incorporated in these analysis including gravity. Then, as presented just below, we adopt another assumption of the shocked slab to clarify its dynamical stability.

In the current paper, we investigate the instability of a plane-parallel slab with finite thickness, which slab is bound by thermal pressure on one side and by ram pressure of the shock on the other side. The pressures on the two sides are dissimilar. We assume incompressibility for the equation of state of the post shock layer (i.e. in the slab), though we assume compressible fluid at the shock surface. This assumption of incompressibility can be suitable, since highly compressed isothermal fluid behaves just like an incompressible fluid as shown by Elmegreen and Elmegreen (1978). Moreover, as demonstrated by Mac Low and Norman (1993), this approximation may be indicated by the fact that the DSI saturates with transonic transverse flows in the shocked slab. By this assumption we can obtain, in addition, an analytical solution to the perturbation equations, with which we can reveal the precise physics of the instabilities.

In the following sections, we perform the linear perturbation analysis, to study the stability of incompressible slab without self-gravity of the layer in § 2 and with self-gravity in § 3. We discuss the DSI and gravitational instability of incompressible slab in § 4. We also discuss the fragmentation process of the slab in § 5 and summarize our results in the final section.

## 2. The DSI of incompressible slab

In order to investigate the stability of the slab of gas swept up by a shock front, we analyze an infinite, plane-parallel shock wave advances to the negative direction of  $z$ -axis with the velocity of  $V_S$  in a uniform medium of density of  $\rho_e$ . We assume incompressibility of the gas except at the shock front and the density in the dense slab being  $\rho_s$ , and that the dense layer is confined from the rear by hot and tenuous gas with a finite pressure  $P_t$ . As first step, we ignore the self-gravity of the slab to present the dispersion relation of the pure DSI (cf. §2 of Nishi 1992). We assume a coordinate that the unperturbed shock front is at  $z = 0$ . At the boundary  $z = 0$ , we impose shock boundary conditions:

$$[\rho v_{\perp}] = 0, \tag{1}$$

$$[P + \rho v_{\perp}^2] = 0, \quad [\rho v_{\perp} \mathbf{v}_{\parallel}] = 0 \tag{2}$$

where  $\rho$  and  $P$  are the density and the pressure, and  $v_{\perp}$  and  $\mathbf{v}_{\parallel}$  are the velocities of the fluid perpendicular and parallel to the shock surface, respectively. The square brackets denote

the difference of the enclosed quantity across the shock front.

The fluid equations for a general first-order perturbation in the slab are

$$\frac{d\mathbf{v}_1}{dt} = -\nabla \left( \frac{P_1}{\rho_s} \right), \quad (3)$$

$$-\nabla \cdot (\rho_s \mathbf{v}_1) = 0, \quad (4)$$

where  $P$  is the pressure of the fluid, and the subscripts 0 and 1 refer to unperturbed and perturbed quantities, respectively. All perturbed quantities are proportional to  $e^{i(kx+\omega t)}$ , then we can rewrite equations (3) and (4) as

$$\{i\omega + (u\partial_z)\} v_{1x} - ik \left( \frac{P_1}{\rho_s} \right) = 0, \quad (5)$$

$$\{i\omega + (u\partial_z)\} v_{1z} - \partial_z \left( \frac{P_1}{\rho_s} \right) = 0, \quad (6)$$

$$ikv_{1x} + \partial_z v_{1z} = 0, \quad (7)$$

where  $u(= (\rho_e/\rho_s)V_S)$  is  $v_0$  in the slab and  $v_{1x}$  and  $v_{1z}$  are the  $x$ - and  $z$ - components of  $\mathbf{v}_1$ , respectively.

According to Vishniac & Ryu (1989), we get the following three (approximate) solutions with two different assumptions. For first set of them, we assume that  $u\partial_z \ll i\omega$ . Then, we can ignore the terms in parentheses and find a combination of the two independent solutions given by

$$P_1 = P_+ e^{kz} + P_- e^{-kz}, \quad (8)$$

$$v_{1x} = -\frac{k}{\omega} \frac{P_+}{\rho_s} e^{kz} - \frac{k}{\omega} \frac{P_-}{\rho_s} e^{-kz}, \quad (9)$$

$$v_{1z} = \frac{ik}{\omega} \frac{P_+}{\rho_s} e^{kz} - \frac{ik}{\omega} \frac{P_-}{\rho_s} e^{-kz}. \quad (10)$$

To find third solution, we consider the case that the perturbed quantities have large gradient and  $u\partial_z$  terms are important. By inspection the third solution is

$$\frac{P_1}{\rho_s} = 0, \quad (11)$$

$$v_{1x} = A \exp \left[ -\frac{i\omega}{u} z \right], \quad (12)$$

$$v_{1z} = \frac{Auk}{\omega} \exp\left[-\frac{i\omega}{u}z\right]. \quad (13)$$

Since we are interested in only the case that perturbation grows, we assume that  $-i\omega_I \gg H/u$  where  $H$  is a thickness of the shocked slab and  $-i\omega_I$  means a growth rate of the perturbation.

We shall determine the boundary conditions. Assuming the very high compressibility at the shock surface, we can suppose  $P_S = \rho_e V_S^2$ . Thus, for the pressure boundary conditions, we integrate the equation of hydrostatic equilibrium (Goldreich & Lynden-Bell 1965), and find them to the first order;

$$P_1(0) = (1 - \beta) \frac{P_S}{\sigma_0} \rho_s \eta - 2\rho_e V_S v_{1z}(0), \quad (14)$$

$$P_1(H) = (1 - \beta) \frac{P_S}{\sigma_0} \rho_s \zeta, \quad (15)$$

where  $\beta (\equiv P_t/P_S)$  is the pressure ratio at the surface of the slab,  $\sigma_0$  is a surface density of the slab,  $\eta (\equiv z_{s1} - 0)$  and  $\zeta (\equiv z_{t1} - H)$  are the displacements of the shock and trailing surfaces, respectively. With the shock boundary conditions, we set the following boundary condition

$$v_{1x}(0) = \frac{k}{\omega} V_S v_{1z}(0). \quad (16)$$

Applying the boundary conditions, we have

$$P_+ + P_- e^{-2kH} = (1 - \beta) \frac{c^2}{H^2 \omega^2} kH (P_+ - P_- e^{-2kH}), \quad (17)$$

$$\frac{P_+}{\rho_s} + \frac{P_-}{\rho_s} = (1 - \beta) \frac{c^2}{H^2 \omega^2} kH \left( \frac{P_+}{\rho_s} - \frac{P_-}{\rho_s} - iAu \right), \quad (18)$$

$$\left( 1 - \frac{c^2 k^2}{\omega^2} \right) A = \frac{iV_S k^2}{\omega^2} \left( \frac{P_+}{\rho_s} - \frac{P_-}{\rho_s} \right), \quad (19)$$

where  $c^2 \equiv uV_S = \rho_e V_S^2 / \rho_s$ .

Then we find the dispersion relation as

$$\omega^2 = \frac{c^2}{H^2} \left[ \frac{k^2 H^2}{2} \pm kH \left\{ \frac{k^2 H^2}{4} - (1 - \beta) \coth[kH] kH + (1 - \beta)^2 \right\}^{1/2} \right]. \quad (20)$$

The numerical estimate of (20) is presented in figure 1, where the growth rate is normalized by  $c/H$ , that is,  $\Omega = \omega/(c/H)$ . The wave-number is expressed as  $K = kH$  and  $\beta = 0.5$  is adopted in the same figure. As clearly shown in this figure, we can find that there is a set of DSI-mode (the other set is damping mode).

We evaluate the limiting case of long wave length ( $kH \rightarrow 0$ ). In the case of  $\beta(1-\beta) \neq 0$ , we have the growth rate as

$$\frac{\Gamma}{c/H} \simeq 2^{-1/2} \beta^{1/4} (1-\beta)^{1/4} (kH)^{1/2}. \quad (21)$$

This growth rate is equal to the long wave length limit of equation (2.35) of Nishi(1992) with the assumption of  $H = \sigma_0/\rho_s$ .

### 3. The DSI of incompressible slab with self-gravity

With the effect of self-gravity, the equation of fluid motion for a general first-order perturbation is

$$\frac{d\mathbf{v}_1}{dt} = \nabla \left( \psi_1 - \frac{P_1}{\rho_s} \right), \quad (22)$$

where  $\psi_1$  is a perturbed component of the gravitational potential. All perturbed quantities are also set to be proportional to  $e^{i(kx+\omega t)}$  in this section. Then we can rewrite equations with  $\psi_1$  as

$$\{i\omega + (u\partial_z)\} v_{1x} + ik \left\{ \psi_1 - \frac{P_1}{\rho_s} \right\} = 0, \quad (23)$$

$$\{i\omega + (u\partial_z)\} v_{1z} + \partial_z \left\{ \psi_1 - \frac{P_1}{\rho_s} \right\} = 0, \quad (24)$$

$$ikv_{1x} + \partial_z v_{1z} = 0. \quad (25)$$

As performed in the previous section, we assume that  $u\partial_z \ll i\omega$  firstly. Namely, we ignore the advection terms then find a combination of the two independent solutions given by

$$\psi_1 = \psi_+ e^{kz} + \psi_- e^{-kz}, \quad (26)$$

$$P_1 = P_+ e^{kz} + P_- e^{-kz}, \quad (27)$$

$$v_{1x} = -\frac{k}{\omega} \left( \frac{P_+}{\rho_s} - \psi_+ \right) e^{kz} - \frac{k}{\omega} \left( \frac{P_-}{\rho_s} - \psi_- \right) e^{-kz}, \quad (28)$$

$$v_{1z} = \frac{ik}{\omega} \left( \frac{P_+}{\rho_s} - \psi_+ \right) e^{kz} - \frac{ik}{\omega} \left( \frac{P_-}{\rho_s} - \psi_- \right) e^{-kz}. \quad (29)$$

Next, since we are concerned for the large gradient of perturbed quantities, we must treat the  $u\partial_z$ -terms. By inspection, this third solution is found as

$$\frac{P_1}{\rho_s} - \psi_1 = 0, \quad (30)$$

$$v_{1x} = A \exp \left[ -\frac{i\omega}{u} z \right], \quad (31)$$

$$v_{1z} = \frac{Auk}{\omega} \exp \left[ -\frac{i\omega}{u} z \right]. \quad (32)$$

Since we are interested in only the case that perturbation grows, we assume that  $-i\omega_I \gg H/u$  again.

We must determine the boundary conditions. We have the perturbed column densities induced by the displacement of the surface as

$$\sigma_s = -\rho_s \eta e^{-kz} e^{i(kx+\omega t)}. \quad (33)$$

$$\sigma_t = \rho_s \zeta e^{-kz} e^{i(kx+\omega t)}, \quad (34)$$

Since the fluid is incompressible, we can determine potential perturbation,  $\psi_1$ , from the surface density distributions  $\sigma_s$  and  $\sigma_t$  alone. With the constraints  $\eta, \zeta \ll 2\pi/k$ , we have the potentials due to  $\sigma_s$  and  $\sigma_t$  as

$$\psi_{\sigma_s} = -\frac{2\pi G \rho_s}{k} \eta e^{-kz} e^{i(kx+\omega t)}, \quad (35)$$

$$\psi_{\sigma_t} = \frac{2\pi G \rho_s}{k} \zeta e^{k(z-H)} e^{i(kx+\omega t)}. \quad (36)$$

From the equations (26), (35), and (36) we find

$$\psi_+ = \frac{2\pi G \rho_s}{k} \zeta e^{-kH}, \quad (37)$$

$$\psi_- = \frac{2\pi G \rho_s}{k} \eta. \quad (38)$$

For the pressure boundary conditions, we find, to first order,

$$P_1(0) = -2\pi G \rho_s^2 H \eta + (1 - \beta) \frac{P_S}{\sigma_0} \rho_s \eta - 2\rho_e V_S v_{1z}(0), \quad (39)$$

$$P_1(H) = 2\pi G \rho_s^2 H \zeta + (1 - \beta) \frac{P_S}{\sigma_0} \rho_s \zeta. \quad (40)$$



Applying the shock boundary conditions gives the next boundary condition

$$v_{1x}(0) = \frac{k}{\omega} V_S v_{1z}(0). \quad (41)$$

Applying the boundary conditions, we get

$$\psi_+ = \frac{2\pi G \rho_s}{\omega^2} \left\{ \left( \frac{P_+}{\rho_s} - \psi_+ \right) - \left( \frac{P_-}{\rho_s} - \psi_- \right) e^{-2kH} \right\}, \quad (42)$$

$$\psi_- = -\frac{2\pi G \rho_s}{\omega^2} \left\{ \left( \frac{P_+}{\rho_s} - \psi_+ \right) - \left( \frac{P_-}{\rho_s} - \psi_- \right) - iAu \right\}, \quad (43)$$

$$\frac{P_+}{\rho_s} + \frac{P_-}{\rho_s} e^{-2kH} = (\tilde{\alpha} + 1) \frac{2\pi G \rho_s kH}{\omega^2} \left\{ \left( \frac{P_+}{\rho_s} - \psi_+ \right) - \left( \frac{P_-}{\rho_s} - \psi_- \right) e^{-2kH} \right\}, \quad (44)$$

$$\frac{P_+}{\rho_s} + \frac{P_-}{\rho_s} = (\tilde{\alpha} - 1) \frac{2\pi G \rho_s kH}{\omega^2} \left\{ \left( \frac{P_+}{\rho_s} - \psi_+ \right) - \left( \frac{P_-}{\rho_s} - \psi_- \right) - iAu \right\}, \quad (45)$$

$$\left( 1 - \frac{c^2 k^2}{\omega^2} \right) A = \frac{iV_S k^2}{\omega^2} \left\{ \left( \frac{P_+}{\rho_s} - \psi_+ \right) - \left( \frac{P_-}{\rho_s} - \psi_- \right) \right\}, \quad (46)$$

where  $\tilde{\alpha} (\equiv (1 - \beta)P_S / (2\pi G \sigma_0^2))$  is the ratio of the deceleration of the whole slab to the acceleration of the slab's self-gravity at the surface.

From equations (42) to (45), we have

$$\begin{aligned} B_+ + B_- &= (\tilde{\alpha} - 1) \frac{2\pi G \rho_s kH}{\omega^2} (B_+ - B_- - iAu) \\ &\quad - \frac{2\pi G \rho_s}{\omega^2} (B_- - B_- e^{-2kH} + iAu), \end{aligned} \quad (47)$$

$$\begin{aligned} B_+ + B_- e^{-2kH} &= (\tilde{\alpha} + 1) \frac{2\pi G \rho_s kH}{\omega^2} (B_+ - B_- e^{-2kH}) \\ &\quad - \frac{2\pi G \rho_s}{\omega^2} (B_+ - B_+ e^{-2kH} + iAu), \end{aligned} \quad (48)$$

where  $B_+ \equiv P_+ / \rho_s - \psi_+$  and  $B_- \equiv P_- / \rho_s - \psi_-$ , respectively. Then we can rewrite equations (47) and (48) as

$$\begin{aligned} &\left\{ \frac{\omega^2}{2\pi G \rho_s} - (\tilde{\alpha} - 1)kH \right\} B_+ \\ &+ \left\{ \frac{\omega^2}{2\pi G \rho_s} + (\tilde{\alpha} - 1)kH + (1 - e^{-2kH}) \right\} B_- \\ &+ \left\{ 1 + (\tilde{\alpha} - 1)kH \right\} iAu = 0, \end{aligned} \quad (49)$$

$$\begin{aligned} & \left\{ \frac{\omega^2}{2\pi G\rho_s} - (\tilde{\alpha} + 1)kH + (1 - e^{-2kH}) \right\} B_+ \\ + & e^{-2kH} \left\{ \frac{\omega^2}{2\pi G\rho_s} + (\tilde{\alpha} + 1)kH \right\} B_- + e^{-2kH} iAu = 0, \end{aligned} \quad (50)$$

and equation (46) as

$$c^2 k^2 B_+ - c^2 k^2 B_- + (\omega^2 - c^2 k^2) iAu = 0. \quad (51)$$

Thus, from equations (49) ~ (51), we have dispersion relation

$$\begin{aligned} \omega^6 & + 2\pi G\rho_s \left\{ 2 - \frac{\tilde{\alpha}}{1-\beta} k^2 H^2 - 2 \coth[kH] kH \right\} \omega^4 \\ & + (2\pi G\rho_s)^2 \left\{ (\tilde{\alpha} + 1) \frac{\tilde{\alpha}}{1-\beta} \coth[kH] k^3 H^3 \right. \\ & - \frac{\tilde{\alpha}}{1-\beta} k^2 H^2 - (\tilde{\alpha}^2 - 1) k^2 H^2 \\ & \left. - 2kH + (1 - e^{-2kH}) \right\} \omega^2 = 0. \end{aligned} \quad (52)$$

We neglect the mode of  $\omega = 0$ , because of the assumption of  $-i\omega_I \gg H/u$ . Finally, then, we obtain the dispersion relation :

$$\begin{aligned} \frac{\omega^2}{2\pi G\rho_s} & = \frac{\tilde{\alpha}}{1-\beta} \frac{k^2 H^2}{2} + \coth[kH] kH - 1 \\ & \pm \left\{ \left( \frac{\tilde{\alpha}}{1-\beta} \frac{k^2 H^2}{2} + \coth[kH] kH - 1 \right)^2 \right. \\ & - (1 + \tilde{\alpha}) \frac{\tilde{\alpha}}{1-\beta} \coth[kH] k^3 H^3 \\ & \left. + \frac{\tilde{\alpha}}{1-\beta} k^2 H^2 - (1 - \tilde{\alpha}^2) k^2 H^2 + 2kH + (e^{-2kH} - 1) \right\}^{1/2}. \end{aligned} \quad (53)$$

#### 4. Discussions

First, we investigate the limiting cases of the dispersion relation of equation (53). To the limit of the long wavelength, that is  $kH \rightarrow 0$ , we have

$$\frac{\omega^2}{2\pi G\rho_s} \simeq \pm kH(1 - \alpha^2)^{1/2}, \quad \alpha \equiv \left( \frac{\beta}{1-\beta} \right)^{1/2} \tilde{\alpha}. \quad (54)$$

From equation (54), we can classify the characteristics of the instability by  $\alpha$ . In the case of  $\alpha > 1$ , the layer is overstable for long wavelength perturbation. When the self-gravity of

the slab does not play important roles, that is, in the limits of  $\tilde{\alpha}$  and  $\alpha \rightarrow \infty$ , we have the dispersion relation of (20). On the other hand, in the case of  $\alpha < 1$ , the layer is unstable for gravity modes.

The numerical presentation of (53) is given in figures 2-4, where the growth rate is normalized by  $(2\pi G\rho_s)^{0.5}$ , that is,  $\Omega = \omega/(2\pi G\rho_s)^{0.5}$ . The wave-number is expressed as  $K = kH$  in all the three figures. In figure 2, we display the cases of  $\alpha = 1.2$  and  $\beta = 0.2, 0.4, 0.6$  and  $0.8$ . Similarly to figure 1, thus, we find the DSI dispersion relations in figure 2. For the same value of  $\alpha$ ,  $\beta$  is the larger, the unstable region becomes the narrower and the growth rate becomes the smaller. This is because large  $\beta$  means inefficiency of the deceleration at the surface of the slab. In the case of the adopted parameters, there is not instability due to the self-gravity.

In figure 3, the dispersion relations of  $\alpha = 0.7$  and  $\beta=0.2, 0.4, 0.6$  and  $0.8$  are presented. Since  $\alpha$  is smaller than unity, we expect the gravitational instability in a range of small wavenumbers. Indeed, we find the gravitational instability for all  $\beta$  in a range of small  $K$ . As indicated in this figure, the growth rate of the gravitational instability depends almost only on  $\alpha$ . On the other hand, we also obtain the DSI in larger  $K$  except the case of  $\beta = 0.8$ . We find again that the growth rate of the DSI does not depend only on  $\alpha$  but also on  $\beta$ . By the way, we want to comment here that for all of the three cases ( $\beta = 0.2, 0.4$  and  $0.6$ ) is stable in the middle of  $K$  in figure 3, that is, both of the DSI and gravitational instability do not occur for a special range of wave-numbers. For the case of  $\beta = 0.8$ , moreover, the DSI mode is always stable because of small  $\tilde{\alpha}$ . These points are the result of the analysis incorporating the structure of the shocked slab, then, it does not appear in Nishi (1992).

In figure 4, we present the dispersion relation for  $\tilde{\alpha} = \alpha = 0$ . As clearly shown in the solid lines, there is only gravitational instability. In other words, we get no DSI mode. Thus, for the case of  $\tilde{\alpha}$ ,  $\alpha \rightarrow 0$ , the self-gravity controls the instability mainly. Indeed, if  $\tilde{\alpha}$ ,  $\alpha \rightarrow 0$ , we obtain

$$\omega^2 = 2\pi G\rho_s \left[ - (1 \pm e^{-kH}) + \frac{(e^{kH/2} \pm e^{-kH/2})^2}{e^{kH} - e^{-kH}} kH \right]. \quad (55)$$

This is the same dispersion relation given by Goldreich and Lynden-Bell (1965). Thus, so long as  $\alpha$  is different from unity somewhat, the order of the growth rate of the gravitational instability becomes  $(G\rho_s)^{-1/2}$  and the scale-length of the most unstable wavelength becomes  $H$  (see also figure 3), which are almost in agreement with the result of Elmegreen and Elmegreen (1978)'s high pressure case. To obtain this mode, it is important to incorporating the structure of the slab.

Next, we display the linear displacements,  $\eta$  and  $\zeta$ , each of which means  $\eta = z_{s1} - 0$

and  $\zeta = z_{t1} - H$ , respectively. Figure 5 shows evolution of the linear displacements for the case of  $\alpha \gg 1.0$  and  $K = 0.24$ . The solid line is  $z_{t1}$  and the dotted line is  $z_{s1}$ . From the upper to lower panels, we display the evolution of the shocked slab at (a)0.0, (b) $1.0 \cdot \delta t$ , and (c) $2.0 \cdot \delta t$  where  $\delta t$  is  $\pi/4|\omega(k = 0.24H)|$ . The unit of the length is  $H$ . We find the bending property of the shocked slab for DSI clearly. On the other hands, figure 6 displays the evolution of the gravitational instability of the shocked slab ( $\tilde{\alpha}$ ,  $\alpha \rightarrow 0$ ). Each of the displayed time is (a)0.0, (b) $1.0 \cdot \delta t$ , and (c) $2.0 \cdot \delta t$ , respectively. The one set of evolution is very different from that of DSI. Someone might think that the shocked slab has evolved nonlinearly. Indeed, the final panels of Fig.5 and Fig.6 shows difficulty of the description of the linear stage. We present both figures only for reader's clear inspection. The essential results of the current discussions are derived from figures 1-4.

Previously, Yoshida & Habe (1992) discussed the nonlinear stage of DSI and gravitational instability under the similar condition adopted in this paper. According to them, the gravitational instability has longer wave-length than DSI. This property is understood through our linear analysis, since the both modes are incompatible in the dispersion relation derived in (53). Thus, our result is in accord with the calculation given by Yoshida & Habe. Someone might think that DSI does not have bending shocked layer since we can not find it clearly in figure 9 of Yoshida & Habe (1992). However, although the thickness of our slab is nearly constant in our linear analysis, in the numerical results of Yoshida & Habe, the shocked slab has a few times larger thickness than the initial value. If the bounding effect were to be more tight in Yoshida & Habe (1992), they would obtain our bending property of DSI in their simulations (cf. Chevalier & Theys 1975).

## 5. Fragmentation of the shocked slab

In the previous considerations, we assume that  $\alpha$  is always constant in each case. But, in reality,  $\alpha$  changes with the evolution of the shocked slab (e.g., Elmegreen 1989). In this section, then, let's discuss the evolution effects (e.g., Nishi 1992). From the definition, we find  $\alpha \propto P_S/\sigma_0^2 \propto (V_S/\sigma_0)^2$ . Since the shocked layer sweeps up the matter, the column density increases and shock velocity decreases with time, hence  $\alpha$  decreases. Thus, the character of the instability in the slab changes at the time  $t = t_{cr}$  when  $\alpha$  becomes unity. In the early stages of the evolution of the shocked layer,  $t < t_{cr}$ , only the DSI can occur in that layer. On the contrary, in the late stages,  $t > t_{cr}$ , it is possible for the shocked layer to be unstable for the DSI (in smaller scale) and the gravitational instability (in larger scale), ordinary. Finally,  $t \gg t_{cr}$ ,  $\alpha$  approaches zero, then the layer becomes stable against the DSI and unstable for the gravitational instability only, as equation (55). In the following

paragraphs, we shall estimate  $t_{\text{cr}}$  and discuss evolution of the shocked slab.

If the shock velocity decreases as  $V_S \propto t^p$  ( $-1 < p < 0$ ), we can estimate  $t_{\text{cr}}$  as follow. Column density at the time of  $t$  is estimated as

$$\sigma_0 = q\rho_e R \quad \text{where} \quad R = \frac{V_S t}{p+1}. \quad (56)$$

Here,  $q$  is the factor depending on the shape of the shock wave, and, of course,  $q = 1$  is the case for the plane shock wave. The distance of the shock surface from the origin is denoted as  $R$ . From the definition of  $t_{\text{cr}}$ ,  $\alpha(t = t_{\text{cr}}) = 1$ , and  $P_S = \rho_e V_S^2$ , we obtain the following relation for  $t_{\text{cr}}$ ;

$$t_{\text{cr}} = \frac{(p+1)\beta^{1/4}(1-\beta)^{1/4}}{q(2\pi G\rho_e)^{1/2}}. \quad (57)$$

Thus,  $t_{\text{cr}}$ , which is the time for the onset of the gravitational instability, does not depend on the initial shock velocity. Although  $\beta$  is a function of time, the product of  $\beta^{1/4}$  and  $(1-\beta)^{1/4}$  depends only very weakly on  $\beta$ . Indeed, for the range of  $\beta = 0.1 - 0.9$ , which is the enough range for realistic situation,  $\beta^{1/4}(1-\beta)^{1/4}$  has only a value in a range from 0.55 to 0.71. Thus, even for a realistic situation, the estimation of  $t_{\text{cr}}$  with the assumption of  $\beta$  being constant is fairly valid. That is to say, we estimate  $t_{\text{cr}}$  as being the order of the free-fall time of the external matter.

In our analysis, the effect of shell expansion is not included. For the case of spherical expansion, the shell expansion effect may be important. The onset time of the gravitational instability is estimated comparing the divergence rate of the expanding shells to the gravitational attraction rate for the expanding shells by Ostriker & Cowie (1981) (in the cosmological case) and by McCray & Kafatos (1987) (in the supershell case). Since we assume large compression ratio at the shock surface, the estimation for the snowplow phase (Eq. (22) of McCray & Kafatos) should be compared with ours. The onset time for this case is somewhat shorter than the free-fall time of the external medium for the typical case. Thus, it may be correct that  $t_{\text{cr}}$  is somewhat shorter than the free-fall time of the external medium even for the expanding shell case, although more detailed investigation is necessary to determine definitely.

Since the DSI saturates with transonic transverse flows in the shocked slab (Mac Low & Norman 1993), only with the effect of the DSI the shocked slab hardly fragments. Thus, we should consider the coupling of the gravitational instability with the DSI for the fragmentation of the evolving shocked layer. First, we consider the most unstable perturbation for the DSI in an early stage ( $t < t_{\text{cr}}$ ). Considering the constant wavelength, the perturbation grows by the DSI, but it may be stable in the later stage as far as the

perturbation is linear (see figures 2-4).<sup>1</sup> Next, we consider the perturbation being unstable for the gravitational instability in the later stages. That perturbation can grow by the DSI in the early stages. Then, the DSI might be related to fragmentation process via the gravity, which occurs in later stages. By the way, importantly, in the intermediate stages, the perturbation becomes stable against both instabilities as shown in figure 3. Then, we find that it is difficult for the DSI directly to connect with the gravitational instability during the evolution of the slab. The calculation by Yoshida & Habe (1992) may suggest the stabilization of the instabilities, that is, the perturbation damps when the wavelength is in this stable range probably because of the evolution effect (e.g., Vishniac 1983, Elmegreen 1989). Thus, as far as the stable range is significant, the effect of the DSI for the structure formation may not be important. However, Yoshida & Habe do not get the growing bending-mode for all parameters, although Mac Low & Norman clearly present the evolution of the bending mode. Thus, there is a possibility that numerical resolution of Yoshida & Habe is not enough. Further investigation including nonlinear stage is necessary.

## 6. Summary

In this paper, we present the dispersion relation of the shocked slab with self-gravity. According to it, when the deceleration dominates the self-gravity, the so-called DSI is efficient. Their growth rates are the function of the scale length which is determined from the efficiency of the deceleration. Thus, we confirm previous researches qualitatively. The slab becomes gravitationally unstable when the gravitational energy is larger than the thermal energy of the layer which is the result of the ram pressure at the shocked surface. In other words, when the deceleration is inefficient, the self-gravity works well. Interestingly, even if the slab is gravitationally unstable in the long wave-length, it is not gravitationally unstable in the short wave-length. Instead of it, the DSI occurs. This suggests that the smaller scale structure than the Jeans-length may be result of the DSI. The growth rate of the gravitational instability depends on almost only  $\alpha$ , while that of the DSI does not depend only on  $\alpha$  but also on  $\beta$ . The growth time-scale of the both instabilities is the order of the free-fall time for the slab density, while the onset-time of the gravitational instability is the order of the free-fall time of the external medium. Thus, within our treatment, the fragmentation by the gravitational instability becomes possible only after about the free-fall time of the external medium. The analytical new point in this paper is that we find stable modes in middle wave-number. This is obtained since we are concerned with the structure of the shocked slab with finite thickness (cf. Nishi 1992). This stable range may suggest

---

<sup>1</sup>Note that  $\alpha$  decreases and  $H$  increases (i.e.  $K$  increases for a constant  $k$ ) with time evolution.

the ineffectiveness of DSI for the fragmentation of the shocked slab via the evolutionary effects (Vishniac 1983; Elmegreen 1989; Yoshida & Habe 1992). Thus, we should determine the structure of the shocked layer when we must study the properties of the instabilities precisely.

We would like to thank the referee, Dr. M.-M. Mac Low, for his valuable comments. We also thank Profs. H. Sato and N. Sugiyama, for their continuous encouragement. HK appreciates the computer maintenance by K. Yoshikawa. This work is supported in part by Research Fellowships of the Japan Society for the Promotion of Science for Young Scientists, No.2780 and 03926 (HK), and by the Japanese Grant-in-Aid for Scientific Research on Priority Areas (No. 10147105) (RN) and Grant-in-Aid for Scientific Research of the Ministry of Education, Science, Sports, and Culture of Japan, No. 08740170 (RN).

## REFERENCES

- Blondin, J. M., & Marks, B. S., 1996, *New Astronomy*, 1, 235  
Chevalier, R.A., & Blondin, J. M., 1995, *ApJ*, 444, 312  
Chevalier, R.A., & Theys, J.C., 1975, *ApJ*, 195, 53  
Dgani, R., van Buren, D., & Noriega-Crespo, A., 1996, *ApJ*, 461, 927  
Elmegreen, B.G., 1989, *ApJ*, 340, 786  
Elmegreen, B.G. & Elmegreen, D.M. 1978, *ApJ*, 220, 1051  
Elmegreen, B.G., & Lada, C.J., 1977, *ApJ*, 214, 725  
Erpenbeck, J. J., 1962, *Phys. Fluids*, 5, 1181  
Goldreich, P. & Lynden-Bell, D., 1965, *MNRAS*, 130, 97  
Grun, J., et . al. 1991, *Phys. Rev. Let.*, 66, 2738  
Ikeuchi, S., 1981, *PASJ*, 33, 211  
Kimura, T., & Tosa, M., 1988, *MNRAS*, 234, 51  
Lubow, S.H., & Pringle, J.E., 1993, *MNRAS*, 263, 701  
Mac Low, M.-M., & Norman, M.L., 1993, *ApJ*, 407, 207  
McCray, R., R. & Kafatos, M., 1987, *ApJ*, 317, 190  
Nagai, T., Inutsuka, S., & Miyama, S.M., 1998, *ApJ*, 506, 306  
Nakano, T., Hasegawa, T., & Norman, C., 1995, *ApJ*, 450, 183

- Nishi, R., 1992, *Prog. Theor. Phys.*, 87, 347
- Ostriker, J.P., & Cowie, L.L., 1981, *ApJ*, 247, L127
- Ryu, D. & Vishniac, E. T., 1987, *ApJ*, 313, 841
- Ryu, D. & Vishniac, E. T., 1988, *ApJ*, 331, 350
- Ryu, D. & Vishniac, E. T., 1991, *ApJ*, 368, 411
- Stevens, I. R., Blondin, J. M., & Pollock, A. M. T., 1992, *ApJ*, 386, 265
- Tomisaka, K., 1990, *ApJ*, 361, L5
- Vishniac, E. T., 1983, *ApJ*, 274, 152
- Vishniac, E. T., 1994, *ApJ*, 428, 186
- Vishniac, E. T., 1995, in *Annals of the New York Academy of Science*, eds Hunter J. H. Jr., and Wilson, R. E., vol. 773, 70
- Vishniac, E. T. & Ryu, D., 1989, *ApJ*, 337, 917
- Voit, G.M., 1988, *ApJ.*, 331, 343
- Welter, G.L. 1982, *A. & Ap.*, 105, 237
- Yoshida, T & Habe, A., 1992, *Prog. Theor. Phys.*, 88, 251



### FIGURE CAPTIONS

Fig.1 — The numerical expression of (20). The growth rate is normalized by  $c/H$ , that is,  $\Omega = \omega/(c/H)$ . In the figure,  $\Omega_r$  is a real part of  $\Omega$ , while  $\Omega_i$  is an imaginary part of  $\Omega$ . The wave-number is expressed as  $K = kH$ . The positive real parts are shown in (a), while the dotted line corresponds to the plus sign of (20) and the solid line to its minus sign. In (b), the two imaginary parts of both the modes coincide.

Fig.2 — The numerical expression of (53). The growth rate is normalized by  $(2\pi G\rho_s)^{0.5}$ . We draw  $\Omega_r$  as a real part of  $\Omega$ , while  $\Omega_i$  as an imaginary part of  $\Omega$ . The wave-number is expressed as  $K = kH$ . We adopt  $\alpha = 1.2$  and  $\beta = 0.2$ (solid),  $0.4$ (dash),  $0.6$ (dot) and  $0.8$ (dot-dash). Only DSI modes are found for the four examples.

Fig.3 — The same figure of Fig. 2 except the value of  $\alpha = 0.7$ . We also adopt  $\beta = 0.2$ (solid),  $0.4$ (dash),  $0.6$ (dot) and  $0.8$ (dot-dash). In small  $K$  we find the gravitational instability, while DSI occurs in large  $K$ . In the middle of  $K$ , we find just the stable modes. The case of  $\beta = 0.8$  does not have DSI even in large range of  $K$ . Of course,  $\Omega_r = 0$  for the gravitationally unstable modes.

Fig.4 — The same figure of Fig. 2 except the value of  $\tilde{\alpha}$ ,  $\alpha = 0.0$ . We find the dispersion relation given in Goldreich and Lynden-Bell (1965). The solid line shows the gravitational instability, while the dotted line is only for the gravitationally modified sound mode.

Fig.5 — The one set of the evolution of the linear displacements are displayed. Here,  $\eta(\equiv z_{s1} - 0)$  and  $\zeta(\equiv z_{t1} - H)$ , then we show  $z_{s1}$  as dotted lines and  $z_{t1}$  as solid lines. Each of the displayed time is (a)0.0, (b) $1.0 \cdot \delta t$ , and (c) $2.0 \cdot \delta t$ . The unit of the length is  $H$ . The bending property of the shocked layer for DSI is found.

Fig.6 — The same figure of figure 5. The displayed times are (a)0.0, (b) $1.0 \cdot \delta t$ , and (c) $2.0 \cdot \delta t$ . The gravitational-unstable slab is presented.

FIGURE 1a

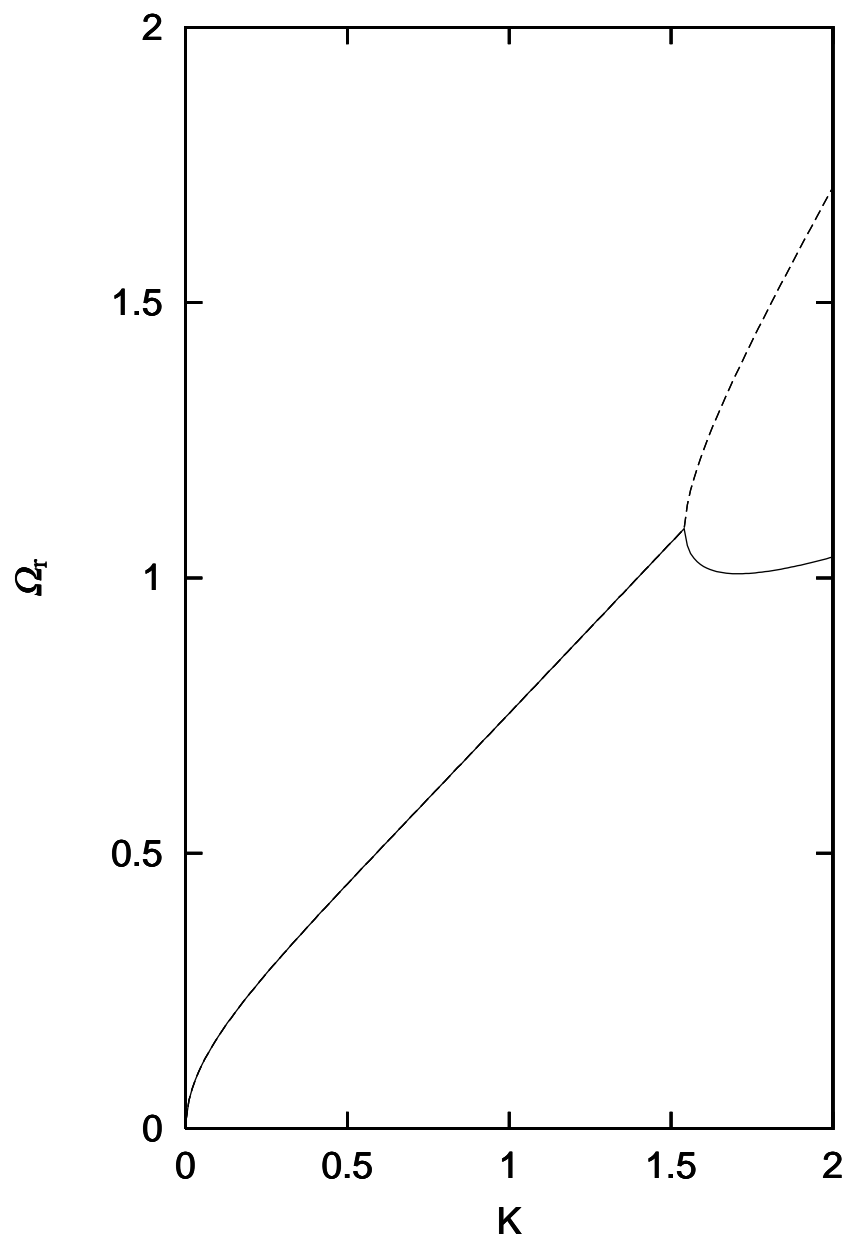


FIGURE 1b

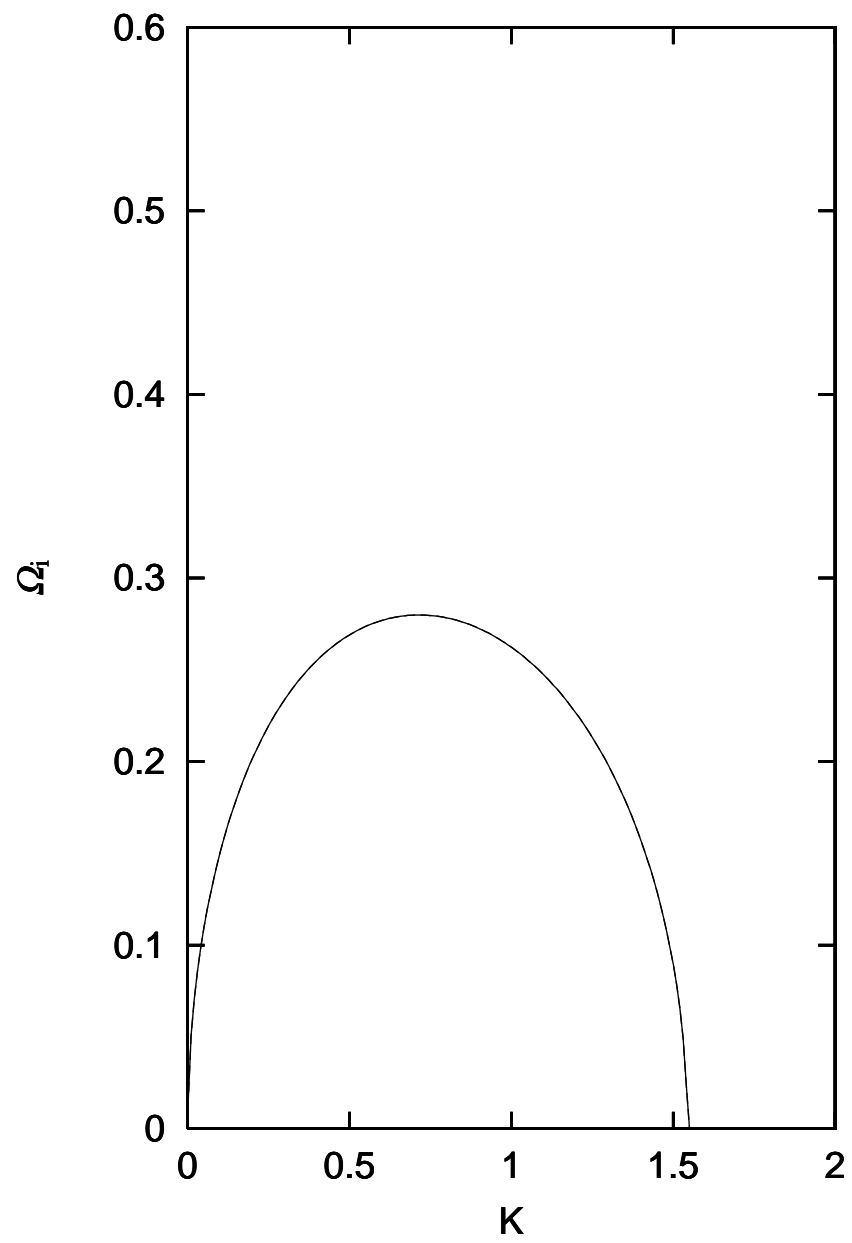


FIGURE 2a

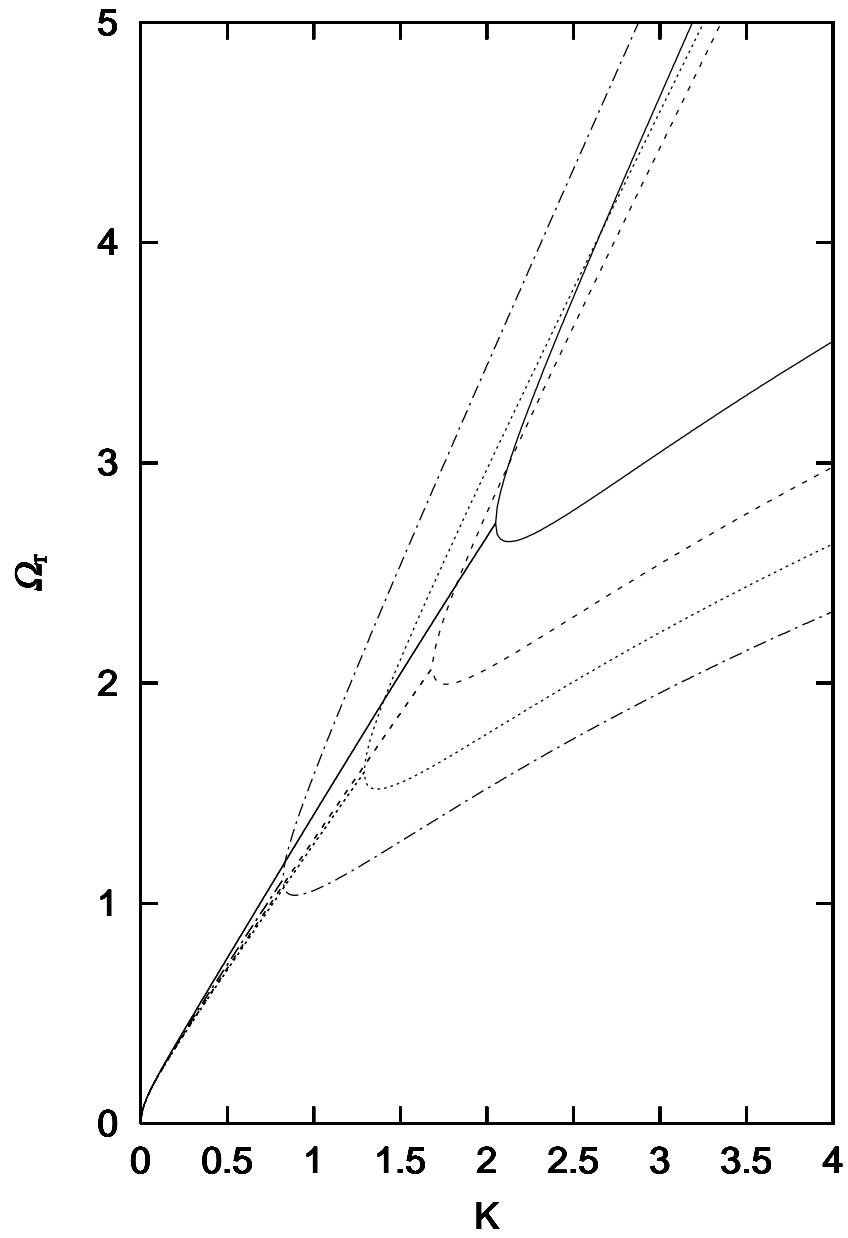


FIGURE 2b

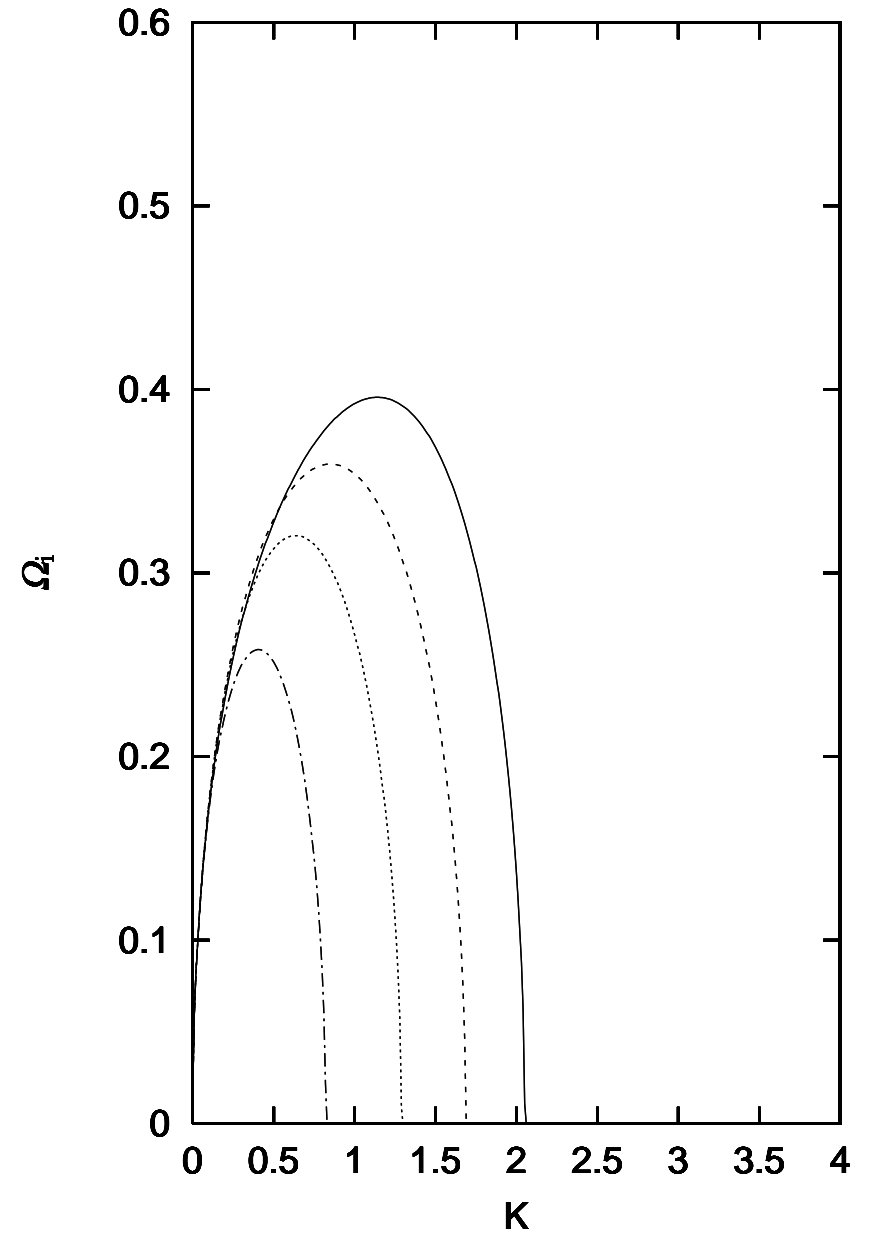


FIGURE 3a

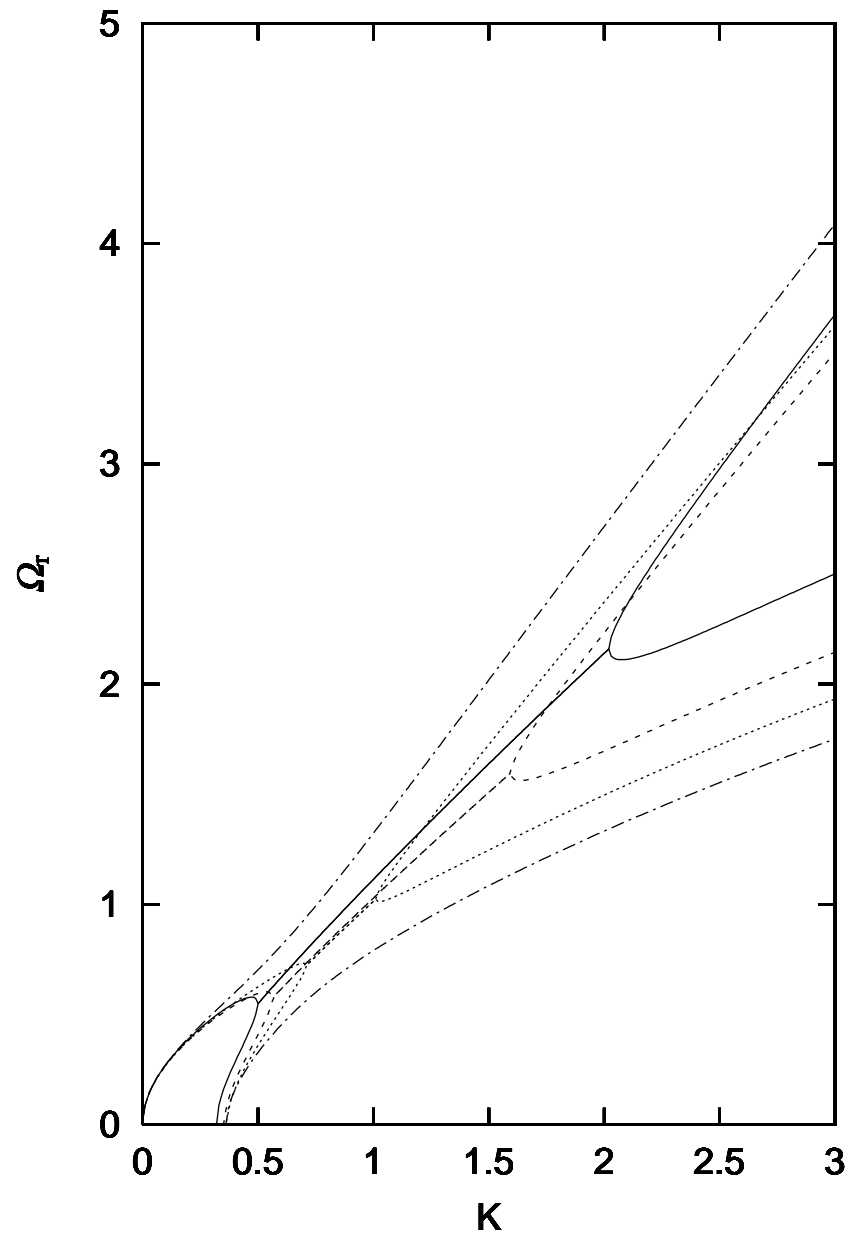


FIGURE 3b

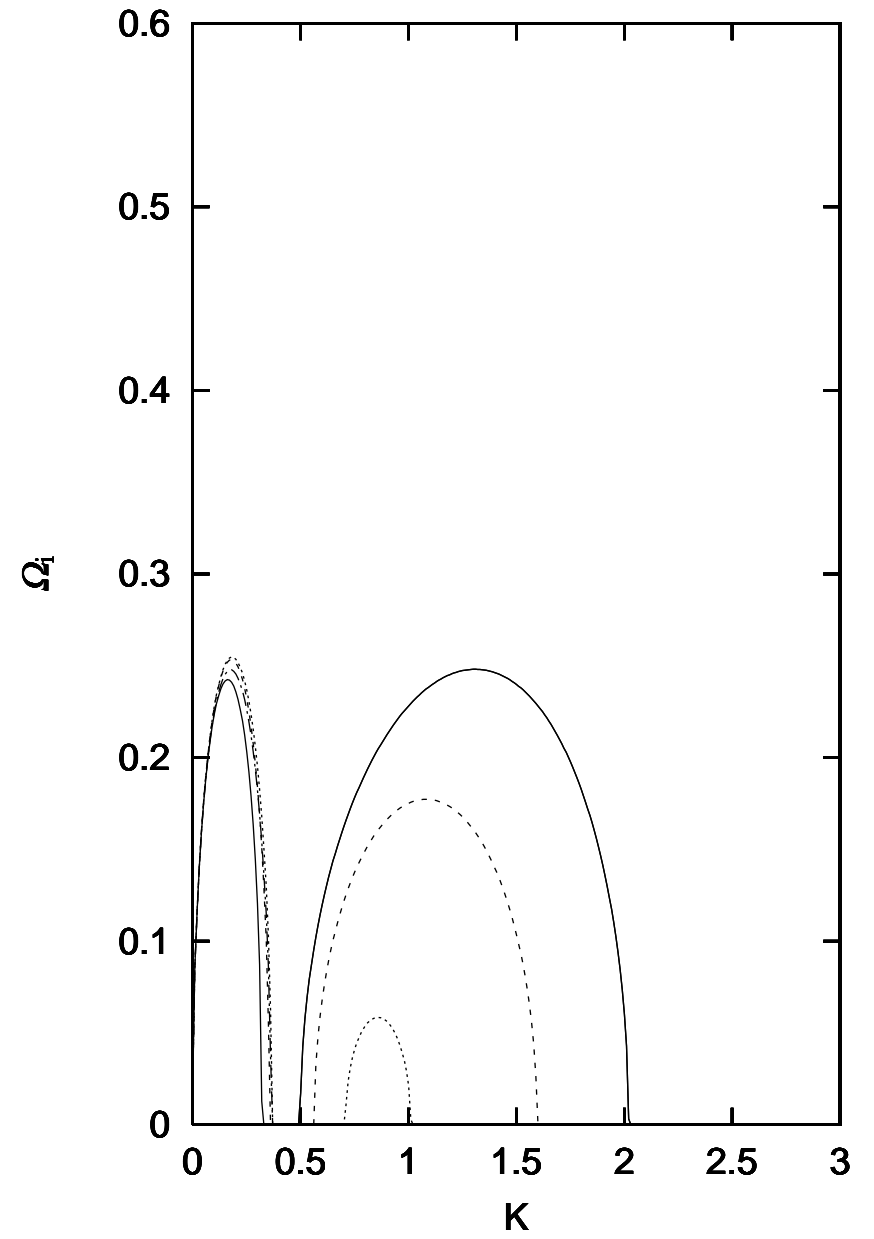


FIGURE 4a

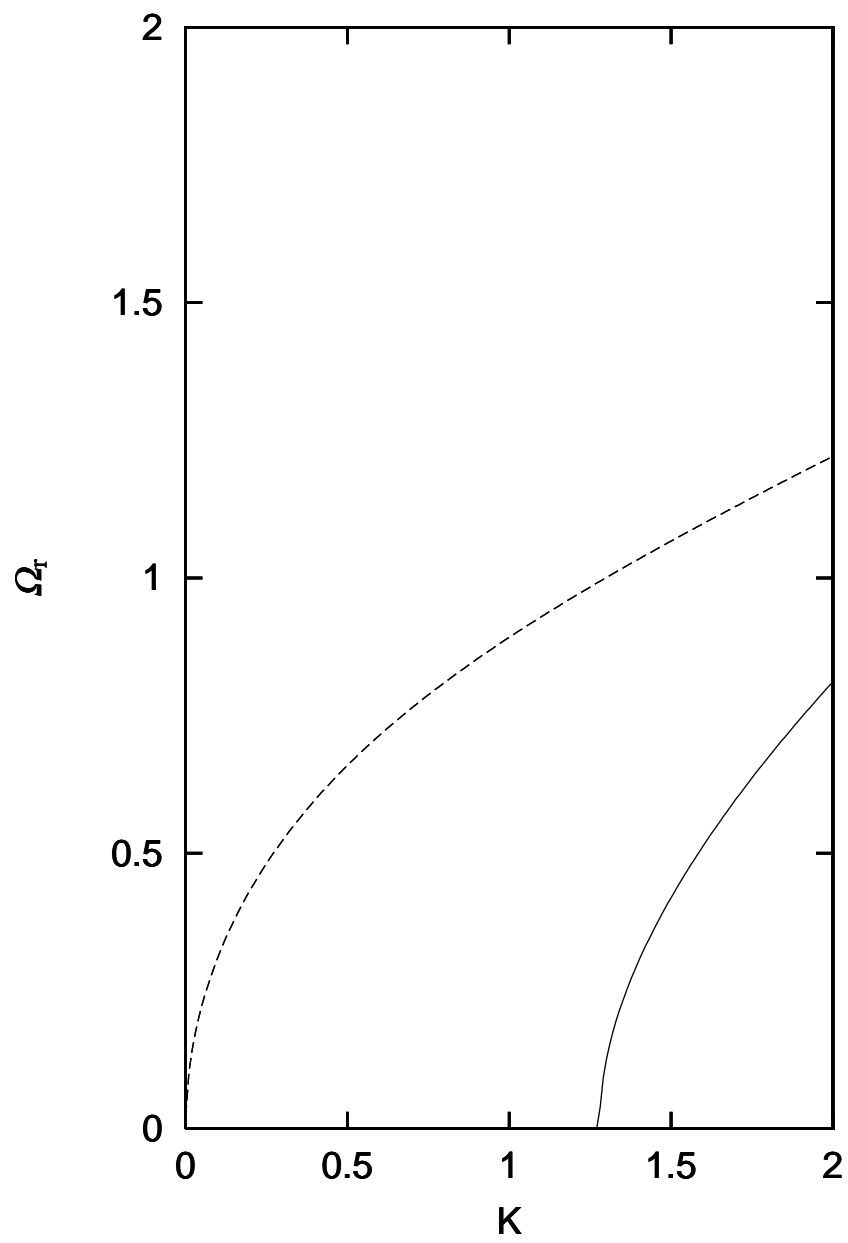


FIGURE 4b

